ELSEVIER

Catalysis Today 42 (1998) 13–23

CATALYSIS TODAY

Mechanistic considerations for the reduction of NO_x over Pt/Al_2O_3 and Al_2O_3 catalysts under lean-burn conditions

R. Burch*, J.A. Sullivan, T.C. Watling

Catalysis Research Centre, Department of Chemistry, University of Reading, Whiteknights, Reading RG6 6AD, UK

Abstract

The reduction of NO_x under lean-burn conditions remains a challenging technical and scientific problem. In this paper, a number of catalytic systems are investigated by steady state testing and temperature-programmed desorption/reaction and the results discussed in terms of the similarities between the reactions in an attempt to rationalise apparently unrelated results. The reaction mechanisms are divided into two classes. (1) Reactions where NO_x reduction occurs on the Pt surface, (e.g. C_3H_6–NO–O_2 reaction over Pt/Al_2O_3) which are active at the lowest temperatures and are resistant to sulphur poisoning. (2) DeNO_x reactions on Al_2O_3 with a weakly adsorbed reductant, (e.g. C_3H_8–NO–O_2 reaction over Pt/Al_2O_3 and Al_2O_3 and the C_3H_8–NO_2–O_2 reaction over Al_2O_3) which are strongly poisoned by sulphur and appear to occur via the formation of a surface nitrate species on the Al_2O_3 which activates the reductant.

Keywords: Al_2O_3 lean-burn conditions; NO_x reduction; Reaction mechanisms; Pt catalysts; SO_2

1. Introduction

Lean NO_x removal is presently receiving considerable research attention. As seen in recent reviews [1,2] many catalyst formulations (e.g. supported noble metals, zeolites with various cations, metal oxides and sulphated metal oxides) have been investigated with various organic reductants (e.g. saturated and unsaturated hydrocarbons, aromatics and alcohols). However, while some empirical progress has been made, there is no acceptable catalyst or catalytic process. It is apparent that a greater understanding of the reaction mechanisms of these catalysts is required to enable further progress in catalyst design to be made.

In this paper results from a series of catalyst systems (viz. C_3H_6–NO–O_2 and C_3H_8–NO–O_2 reactions over Pt/Al_2O_3, and C_3H_8–NO–O_2 and C_3H_8–NO_2–O_2 reactions over Al_2O_3) are presented and the similarities between them highlighted in an attempt to rationalise apparently unrelated results. In particular, the differences in the sulphur resistance of the catalyst systems investigated is presented and discussed in terms of the reaction mechanism. This paper includes results from both steady state catalyst testing and from temperature-programmed desorption and temperature-programmed reaction experiments.

2. Experimental

The γ-alumina used in this study was CK300 (Akzo Chemie, SA=182 $m^2\,g^{-1}$) with a grain size

*Corresponding author.

0920-5861/98/$32.00
PII S0920-5861(98)00072-8

of 250–850 μm. The platinum on γ-alumina catalyst was prepared by incipient wetness impregnation using dinitrodiammine-Pt as the precursor and CK300 as the alumina. The sample was calcined at 500°C for 14 h and had a 1 wt% Pt loading and a dispersion of 71% (by H_2 chemisorption).

Steady state catalyst testing was carried out using a quartz tubular downflow reactor (i.d. 5 mm). The sample (100 mg) was held between plugs of quartz wool. Reactant gases were fed from independent mass flow controllers. The reactant composition is specified in the figure captions. The total flow was 200 cm^3 min^{-1}, corresponding to a space velocity of 87 000 h^{-1}. The reactor outflow was analysed using a Perkin-Elmer Autosystem gas chromatograph with a TCD detector, a Signal Series 2000 IR CO_2 analyser and a Signal Series 4000 chemiluminescence NO_x analyser (for NO and total NO_x (i.e. NO+NO_2)). The chromatograph used a Heysep N column for the separation of CO_2, N_2O, C_3H_6/C_3H_8 and H_2O, and a molecular sieve 13X column for the separation of O_2, N_2 and CO, as described in more detail elsewhere [3]. No reaction was observed over quartz wool, provided the temperature was below 600°C.

Before testing the 1% Pt/Al_2O_3, the catalyst was pretreated for 1 h in the reactant stream at 480°C. The catalyst was then cooled and measurements taken as the temperature was increased stepwise. The catalyst was left at each temperature for long enough for steady state to be reached; usually 10 min was more than sufficient, but with the C_3H_6–NO–O_2 reaction >1 h was required in the region of the light-off as a result of the exotherm generated. The catalyst testing was repeated to verify the results were reproducible.

The catalyst was then sulphated (forming sulphated Pt/Al_2O_3) and tested again. Sulphation was performed by heating to 480°C in flowing air (5 cm^3 min^{-1}). The feed was then changed to 400 ppm SO_2, 4% O_2 in N_2 flowing at 25 cm^3 min^{-1} for 9 h. The sample was then purged for 15 min in flowing air (30 cm^3 min^{-1}) before cooling.

Three sulphated Al_2O_3 samples were also prepared by treating 420 mg of Al_2O_3 with 400 ppm SO_2 and 4% O_2 in N_2 flowing at 25 cm^3 min^{-1} at 500°C for either 9, 22 or 35 h. In the last case a Pt/SiO_2 catalyst at the same temperature was placed upstream of the Al_2O_3 to oxidise SO_2 to SO_3. These samples are designated S1, S2 and S3, respectively.

For the TPD/TP reaction studies the sample (420 mg) was placed in a quartz tube between quartz wool plugs. The reactor outflow was connected by a fast response continuously evacuated capillary to a Fisons Gaslab 300 quadrupole mass spectrometer controlled by a bench top PC. This allowed continuous analysis of the reactor effluent. A thermocouple in contact with the catalyst provided continuous temperature readings to the computer. The NO signal was calculated from the m/e=30 signal allowing for the contribution of NO_2 to this signal using literature cracking patterns for NO_2 [4]. This "correction" was carried out by taking the raw data signal for the m/e=46 peak and multiplying each data point by 2.7 [4] to form a signal corresponding to the m/e=30 contribution from NO_2. Each of these calculated values is then removed from the corresponding m/e=30 value to yield a signal for NO which contains no contribution from NO_2.

The catalyst was oxidised for 2 h at 550°C in a flow of 5% O_2 in He prior to TPD and TP reaction experiments and under the same conditions for 1 h between experiments. For both types of experiment the catalyst was dosed at room temperature in a flow of 1.7% NO and 6.4% O_2 in He for 30 min in order to simulate a dose of NO_2. The sample was purged for 1 h in He to remove physisorbed species. The temperature was ramped at 10°C min^{-1} while the reactor outflow was monitored by the mass spectrometer. In TPD experiments a flow of 98 cm^3 min^{-1} of He was passed over the sample, while 1380 ppm C_3H_8 in He flowing at 113 cm^3 min^{-1} was used for temperature-programmed reaction experiments.

3. Results

3.1. C_3H_6–NO–O_2 *and* C_3H_8–NO–O_2 *reactions over* Pt/Al_2O_3

The effect of temperature on the C_3H_6–NO–O_2 and C_3H_8–NO–O_2 reactions over unsulphated Pt/Al_2O_3 is shown Figs. 1 and 2 (filled points). It is clear that there are a number of differences in behaviour dependent on whether C_3H_8 or C_3H_6 is used as the reductant, viz.,

- C_3H_6 is much more reactive than C_3H_8, 50% hydrocarbon conversion being reached at 250

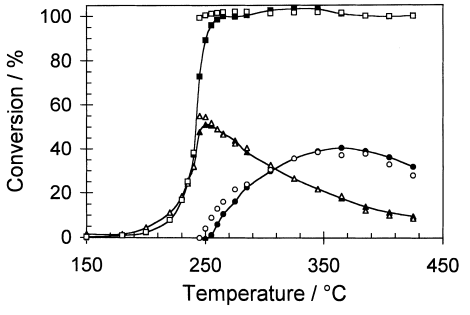

Fig. 1. The effect of temperature on the C_3H_6–NO–O_2 reaction over unsulphated (filled points) and sulphated (open points) 1% Pt/Al_2O_3. Feed: 1000 ppm C_3H_6, 1000 ppm NO and 5% O_2 (■, □ C_3H_6; ▲, Δ NO to N_2 and N_2O; ●, ○ NO to NO_2).

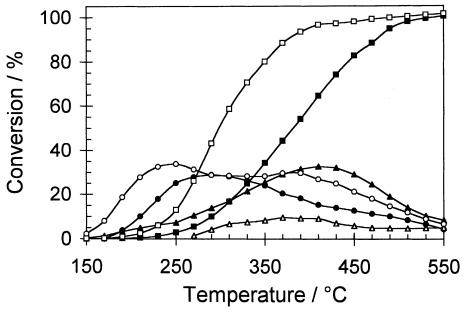

Fig. 2. The effect of temperature on the C_3H_8–NO–O_2 reaction over unsulphated (filled points) and sulphated (open points) 1% Pt/Al_2O_3. Feed: 1000 ppm C_3H_8, 1000 ppm NO and 5% O_2 (■, □ C_3H_8; ▲, Δ NO to N_2 and N_2O; ●, ○ NO to NO_2).

and 380°C, respectively. In addition, C_3H_6 lights-off considerably more rapidly than C_3H_8.

- C_3H_6 is a more effective NO_x reductant and is active at a lower temperature than C_3H_8; C_3H_6 gives a maximum NO_x conversion of 50% at 240°C, compared with 33% at 410°C for C_3H_8.
- Maximum NO_x conversion is coincident with 100% hydrocarbon conversion for C_3H_6 but not for C_3H_8.
- NO_2 is produced at all temperatures above 150°C with C_3H_8, but is only produced with C_3H_6 after 100% hydrocarbon conversion.

The effect of catalyst sulphation on the C_3H_6–NO–O_2 and C_3H_8–NO–O_2 reactions over Pt/Al_2O_3 is shown in Figs. 1 and 2 (open points). The C_3H_6–NO–O_2 reaction is unaffected by sulphation. In contrast, sulphation results in the maximum NO_x conversion of the C_3H_8–NO–O_2 reaction falling from 33% to 10% and in a lowering of the C_3H_8 light-off temperature. The shift in C_3H_8 light-off temperature on sulphation of the Pt/Al_2O_3 catalyst is well known [5].

3.2. C_3H_8–NO–O_2 *and* C_3H_8–NO_2–O_2 *reactions over* Al_2O_3

Since NO_x reduction in the C_3H_8–NO–O_2 reaction over Pt/Al_2O_3 is believed to involve the reaction of NO_2 and C_3H_8-derived species on the Al_2O_3 support and/or at the metal-support interface [6], the C_3H_8–NO–O_2 and C_3H_8–NO_2–O_2 reactions over Al_2O_3 have also been studied. Fig. 3 shows the effect of temperature on the C_3H_8–NO–O_2 reaction over Al_2O_3. Al_2O_3 is much less effective at oxidising C_3H_8 than Pt/Al_2O_3; the temperature required for 50% conversion is much higher with Al_2O_3 (580°C compared with 380°C) and some CO is produced whereas with Pt/Al_2O_3 CO_2 is the only combustion product. Maximum NO_x conversion occurs at a higher temperature relative to Pt/Al_2O_3 (590°C, compared with 410°C). Oxidation of NO to NO_2 occurs after 100% C_3H_8 conversion has been reached.

The effect of temperature on the C_3H_8–NO_2–O_2 reaction over Al_2O_3 is shown in Fig. 4. The oxidation of C_3H_8 to CO and CO_2 is similar to that observed with the C_3H_8–NO–O_2 reaction, except that at lower temperatures (<550°C) the conversion of C_3H_8 is higher at a given temperature in the presence of NO_2 than is the case with NO. Reduction of NO_2 to NO is also observed. However, the major difference between

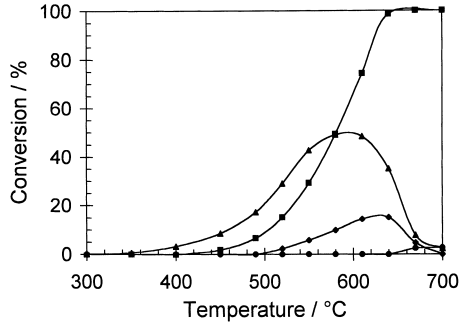

Fig. 3. The effect of temperature on the C_3H_8–NO–O_2 reaction over Al_2O_3. N_2O production was not observed in this experiment. Feed: 1000 ppm C_3H_8, 400 ppm NO and 5% O_2 (■ C_3H_8; ◆ C_3H_8 to CO; ▲ NO to N_2; ● NO to NO_2).

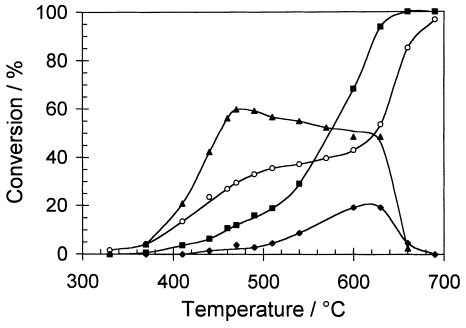

Fig. 4. The effect of temperature on the C_3H_8–NO_2–O_2 reaction over Al_2O_3. N_2O production was not observed in this experiment. Feed: 1000 ppm C_3H_8, 400 ppm NO_2 and 5% O_2 (■ C_3H_8; ◆ C_3H_8 to CO; ▲ NO_2 to N_2; ○ NO_2 to NO).

the C_3H_8–NO_2–O_2 and C_3H_8–NO–O_2 reactions over Al_2O_3 is that NO_x reduction occurs at a much lower temperature with the former reaction (e.g. the temperature for 30% NO_x conversion is shifted by 100°C). Hamada [7] has also observed this increased reactivity of NO_2 compared to NO.

Fig. 5 shows the effect of temperature on the C_3H_8–NO–O_2 reaction over sulphated Al_2O_3 (sample S3). Sulphation results in the C_3H_8 light-off shifting to higher temperature (50% conversion occurring at 625°C, compared with 580°C for the unsulphated sample (Fig. 3)). In addition, no NO_x conversion or CO production is observed with the sulphated sample. Similar, trends have been reported by Hamada et al. [8] for the C_3H_8–NO–O_2 reaction over Al_2O_3 and sulphated Al_2O_3.

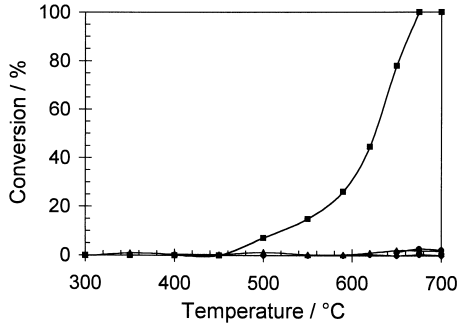

Fig. 5. The effect of temperature on the C_3H_8–NO–O_2 reaction over sulphated Al_2O_3 (S3). N_2O production was not observed in this experiment. Feed: 1000 ppm C_3H_8, 400 ppm NO and 5% O_2 (■ C_3H_8; ◆ C_3H_8 to CO; ▲ NO to N_2; ● NO to NO_2).

3.3. *TPD of* NO *and* NO + O_2 *from* Al_2O_3

The interaction of NO_x with Al_2O_3 is expected to be important for the reduction of NO_x over Al_2O_3 and has therefore been studied by temperature programmed desorption (TPD). The effect of sulphation of the Al_2O_3 has also been investigated.

The *m*/*e*=30 (NO and NO_2) signals from the TPD of Al_2O_3 exposed to either NO or an NO+O_2 mixture are shown in Fig. 6. It is clearly seen that far more NO is adsorbed in the presence of O_2. This is probably due to the adsorption of NO_2, formed in the gas phase, onto the surface and shows how NO_2 is adsorbed in greater quantities on Al_2O_3 relative to NO.

The effect of various SO_2 treatments of the Al_2O_3 on the TPD profiles obtained after pretreatment with NO+O_2 are shown in Figs. 7–9. The *m*/*e*=30 (NO and NO_2) signal (Fig. 7) shows two peaks. Sulphation has a dramatic effect on the second (higher temperature)

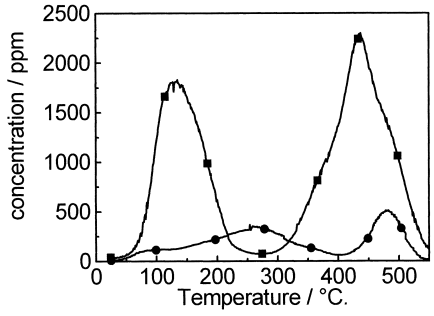

Fig. 6. *m*/*e*=30 (NO and NO_2) signal from TPD of Al_2O_3 preexposed to an [NO+O_2] mixture (■) or to NO (●) at ambient temperature.

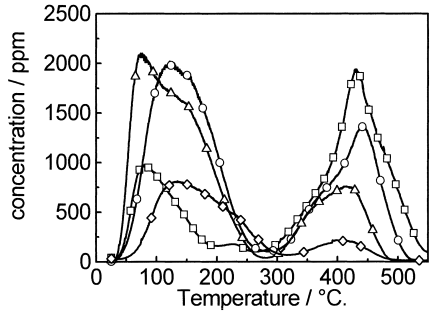

Fig. 7. Comparison of the *m*/*e*=30 (NO and NO_2) traces from TPD of Al_2O_3 samples after exposure to an [NO+O_2] mixture at ambient temperature (□ Al_2O_3, ○ S1, Δ S2, and ◇ S3).

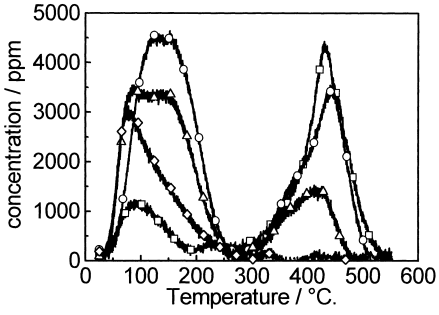

Fig. 8. Comparison of the m/e=46 (NO_2) traces from TPD of Al_2O_3 samples after exposure to an [NO+O_2] mixture at ambient temperature (□ Al_2O_3, ○ S1, Δ S2, and ◇ S3).

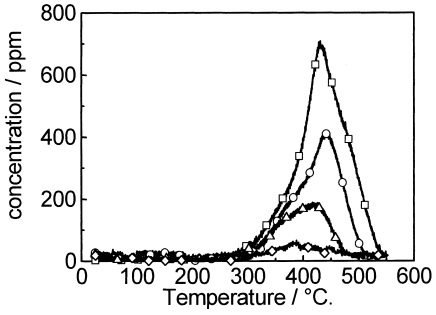

Fig. 9. Comparison of the m/e=32 (O_2) traces from TPD of Al_2O_3 samples after exposure to an [NO+O_2] mixture at ambient temperature (□ Al_2O_3, ○ S1, Δ S2, and ◇ S3).

NO desorption, lowering the total amount of NO desorbed and, in the case of the two most severely sulphated samples (S2 and S3), the temperature of maximum desorption. The area of the first peak is increased relative to untreated Al_2O_3 by sulphation. The ''corrected'' amounts of NO desorbed for each peak, i.e. with allowance made for the contribution of NO_2 to the m/e=30 signal are complied in Table 1. The m/e=46 (NO_2) signal (Fig. 8) exhibits the same trends as the m/e=30 (NO and NO_2) signal.

The m/e=32 (O_2) signal is shown in Fig. 9 and consists of single peak coincident with the second NO desorption peak. This peak decreases in intensity as the degree of sulphation is increased, with the most highly sulphated sample (S3) barely releasing any O_2 (13 μmol g^{-1} compared to 116 μmol g^{-1} for the Al_2O_3 catalyst).

3.4. *Temperature programmed reaction of* Al_2O_3 *with* C_3H_8

The interaction between C_3H_8 and Al_2O_3 has been studied by TP reaction of C_3H_8 with Al_2O_3 both with and without preadsorption of NO+O_2. With untreated

Table 1
Peak areas and positions from TPD experiments on Al_2O_3 and sulphated Al_2O_3 after exposure to an [NO+O_2] mixture

Sample	First peak				Second peak					
	NO		NO_2		NO		NO_2		O_2	
Al_2O_3	80		88		428		430		431	
		117		148		263		503		116
		(54)				(43)				
S1	121		152		441		441		443	
		308		690		176		413		68
		(100)				(53)				
S2	73		84		410		413		416	
		322		581		102		191		36
		(146)				(50)				
S3	75		77		329		332		388	
		214		388		46		4		13
		(57)				(26)				

420 mg of sample was dosed with NO and O_2 at ambient temperature for 30 min and purged in He for 1 h prior to temperature ramp (10°C min^{-1}). Upper left figure is the temperature of peak maximum in °C, while the lower right represents the amount desorbed in μmol g^{-1}. The values in parentheses show the ''corrected'' amount of NO desorbed (see text).

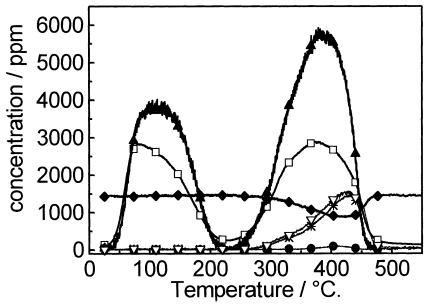

Fig. 10. Temperature programmed reaction profile of C_3H_8 with Al_2O_3 preexposed to an [NO+O_2] mixture at ambient temperature. Feed: 1380 ppm C_3H_8 (■ NO and NO_2, ● O_2, ▲ NO_2, ◆ C_3H_8, * CO_2 and N_2O and ∇ CO and N_2).

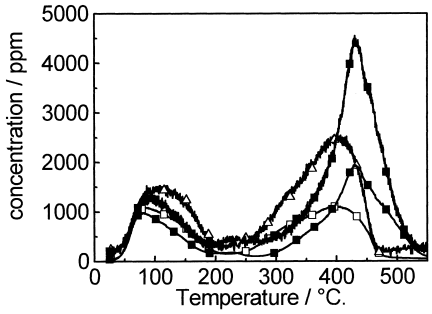

Fig. 11. Desorption profiles of Al_2O_3 preexposed to an [NO+O_2] mixture at ambient temperature in the presence (open points) and absence (filled points) of $C_3H_{8\ (g)}$ (■, □ *m/e*=30 (NO and NO_2); ▲, Δ *m/e*=46 (NO_2)).

Al_2O_3, no uptake of C_3H_8 was observed during the temperature ramp (results not shown), nor was any carbon found to be deposited on the Al_2O_3 after the experiment, indicating that C_3H_8 does not interact with Al_2O_3 in the absence of preadsorbed NO_x.

Fig. 10 shows the TP reaction profile obtained in the presence of 1380 ppm C_3H_8 from Al_2O_3 preexposed to NO+O_2. Peak areas are given in Table 2. The *m/e*=30 (NO and NO_2), *m/e*=46 (NO_2) and *m/e*=32 (O_2) profiles differ from those obtained in the absence of C_3H_8. Fig. 11 compares the NO and NO_2 desorptions in the presence and absence of C_3H_8. The sulphated Al_2O_3 samples exhibited similar trends (not shown). The magnitude and position of the first NO/NO_2 desorption (*m/e*=30) peak (Fig. 11) remains rather unaffected by the presence of the gaseous hydrocarbon, just as the hydrocarbon trace (*m/e*=29) is unaffected by the NO/NO_2 desorption (Fig. 10). However the second NO/NO_2 desorption peak begins at around 250°C, i.e. roughly 50°C lower than in the absence of C_3H_8. The peaks are also generally smaller and arrive at their maximum value at lower temperatures when C_3H_8 is present. Similarly, Shimokabe et al. [9] report the temperature for NO_x

Table 2
Peak areas and positions from TP reaction experiments on Al_2O_3 and sulphated Al_2O_3 in the presence of 1380 pm C_3H_8 after exposure to an [NO+O_2] mixture

Sample	First peak				Second peak										CO_2^*
	NO			NO_2			NO			NO_2			O_2		N_2O/CO_2		N_2/CO		
Al_2O_3	82			86			395			399			413		423		425		
		144			172			213			382			12		178			269	3.8
		(108)						(92)											
S1	132			153			378			378			—		401		391		
		385			688			169			259					74			86	1.8
		(174)						(90)											
S2	73			84			341			334			—		347		358		
		358			625			90			144					58			66	1
		(165)						(59)											
S3	81			96			298			334			—		309		299		
		215			331			52			—					17			20	—
		(128)						(38)											

420 mg of sample was dosed in NO and O_2 at ambient temperature for 30 min and purged in He for 1 h prior to switching in C_3H_8 and temperature ramping (10°C min^{-1}). Upper left figure is the temperature of peak maximum in °C, while the lower right figure is the amount desorbed in μmol g^{-1}. The values in parentheses show the "corrected" amount of NO desorbed (see text). CO_2^* represents CO_2 formed from oxidation of the sample at 550°C after completion of the TP experiment.

desorption from Cu-mordenite and CuO samples to be lowered by the presence of hydrocarbons.

The C_3H_8 signal also begins to decrease at about 250°C and reaches a minimum at a temperature of 410°C before rising again to its original level at higher temperatures. This decrease in the C_3H_8 signal is mirrored by rises in signals at *m/e*=28 and *m/e*=44 which are due to the formation of CO/N_2 and CO_2/N_2O, respectively. These peaks (after being corrected for gas phase C_3H_8 contributions) reach their maximum at a temperature of 410°C, i.e. the same temperature at which the C_3H_8 consumption is highest. The O_2 signal from this experiment is much reduced in the presence of C_3H_8. It peaks at around 400°C and corresponds to the release of 12 μmol g^{-1} (Table 2) compared to 116 μmol g^{-1} O_2 in the absence of C_3H_8 (Table 1).

C_3H_8 TP reaction experiments with sulphated Al_2O_3 after preexposure to $NO+O_2$ exhibit similar trends to Al_2O_3, i.e. a decrease in C_3H_8 signal coincident with the second NO/NO_2 peak, a shift in the second desorption peak to lower temperature and the concomitant formation of peaks attributable to CO/N_2 and CO_2/N_2O (Table 2). However, the amounts of such reaction products formed decreases with increasing sulphation of the catalyst (as does the amount of C_3H_8 consumed). This can be seen in Fig. 12 in which the *m/e*=44 formation profiles obtained are plotted for each of the Al_2O_3 and sulphated Al_2O_3 samples. It is also notable that no O_2 was evolved from the sulphated Al_2O_3 during these experiments, presumably as a result of reaction between any O_2 released and C_3H_8 to give CO and CO_2, coupled with the fact that the amount of O_2 available to desorb (in the absence of C_3H_8) decreases with increasing severity of sulphation. The values presented in Table 2 for the species present at *m/e*=28 and 44 can be calculated as a sum due to the fact that both CO and N_2 and CO_2 and N_2O have the same response factors in the mass spectrometer. Unfortunately it was not possible to deconvolute these signals but it should be noted that we can take their aggregate values to be an indication of the amount of interaction between the gas phase and the surface. The higher the level of sulphation the lower the amount of adsorbed NO_x and thus the lower the interaction seen between the surface and the $C_3H_{8\,(g)}$.

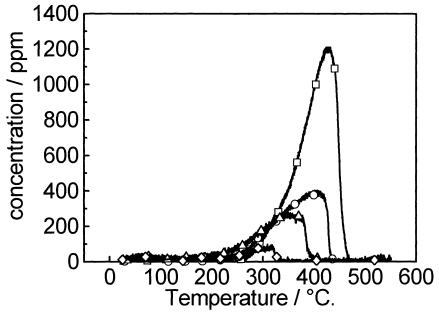

Fig. 12. *m/e*=44 (N_2O and CO_2) profiles formed from reaction of $C_3H_{8\,(g)}$ with Al_2O_3 samples preexposed to an $[NO+O_2]$ mixture. (□ Al_2O_3, ○ S1, Δ S2, ◇ S3)

4. Discussion

The mechanism of NO_x reduction depends on both the catalyst and the reductant used. Thus, there is not a single mechanism for NO_x reduction. The effect of sulphur on the $DeNO_x$ reactivity will depend on the mechanism and hence on the catalyst and reductant used. Experimental results on a number of $DeNO_x$ systems have been presented above, viz. the C_3H_6–NO–O_2 and C_3H_8–NO–O_2 reactions over Pt/Al_2O_3 and the C_3H_8–NO–O_2 and C_3H_8–NO_2–O_2 reactions over Al_2O_3. These results are now discussed in terms of some common features linking these reactions together and on the different mechanisms occurring.

The C_3H_6–NO–O_2 and C_3H_8–NO–O_2 reactions over unsulphated Pt/Al_2O_3 (Figs. 1 and 2) show a number of differences suggesting that the reaction mechanism depends on the choice of reductant. Indeed, on the basis of detailed kinetic studies [6,10] different mechanisms for these two reactions have been proposed. These mechanisms are summarised in Figs. 13 and 14.

With the C_3H_6–NO–O_2 reaction (Fig. 13), the Pt surface is predominately covered by carbonaceous species derived from C_3H_6, while the coverage of oxygen is negligible. The oxidation of NO to NO_2 is not observed in the presence of C_3H_6 due to the lack of oxygen on the Pt surface. NO reduction occurs by the dissociation of adsorbed NO at vacant Pt sites, followed by the combination of adsorbed N and NO to form either N_2 or N_2O. This mechanism is supported by our earlier TAP study [11]. Note that the reaction appears to occur exclusively on the Pt surface.

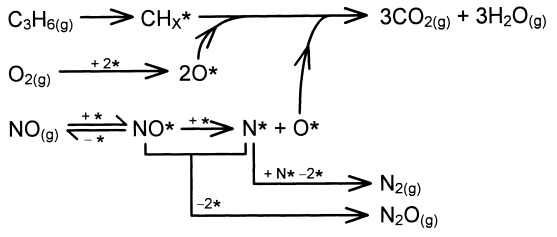

Fig. 13. Proposed mechanism for the C_3H_6–NO–O_2 reaction. All reactions occur on the Pt surface. * indicates a site on the Pt surface.

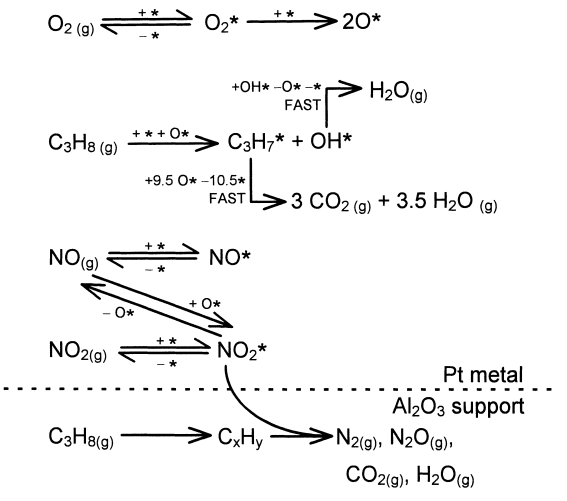

Fig. 14. Proposed mechanism for the C_3H_8–NO–O_2 reaction. * indicates a site on the Pt surface. Reactions above the dotted line occur on the Pt surface, while reactions below occur on the Al_2O_3 support. The reaction between NO_2^* and C_xH_y is believed to take place at the metal-support interface.

In contrast, with the C_3H_8–NO–O_2 reaction (Fig. 14), the coverage of oxygen on the Pt surface is high, while that of C_3H_8-derived species is negligible. This difference between C_3H_8 and C_3H_6 is due to the former being much less effective at removing adsorbed oxygen from the metal surface. The high coverage of oxygen results in oxidation of NO to NO_2 over a wide temperature range and even in the presence of the reductant. NO reduction appears to occur by a mechanism in which NO_2, formed by oxidation of NO on the Pt surface, migrates to the metal-support interface where it reacts with C_3H_8-derived species. This conclusion was based on the fact that in our kinetic studies [6] the rate of NO_x reduction correlated with the calculated coverage of NO_2 on the Pt surface suggesting a mechanism involving interfacial NO_2.

Several attempts were made to fit the kinetic data to a number of other models based on mechanisms proposed in the literature, including ones involving gas phase NO_2, but none were found to fit the data satisfactorily. In this case dissociation of NO on the Pt surface does not appear to occur, presumably because it is inhibited by the high oxygen coverage on the Pt surface.

It is also worth noting the effect of changing the support on the C_3H_6–NO–O_2 and C_3H_8–NO–O_2 reactions on supported Pt. With C_3H_6, changing the support from Al_2O_3 to SiO_2 results in the hydrocarbon light-off, and the temperature of maximum NO_x conversion, shifting to lower temperatures for samples of comparable metal dispersion [12]. In addition, the maximum NO_x conversion is higher with Pt/SiO_2. The lower hydrocarbon light-off temperature obtained with Pt/SiO_2 compared to Pt/Al_2O_3 has also been reported for hydrocarbon combustion (i.e. in the absence of NO_x) and has been attributed, in the case of Pt/Al_2O_3, to the strong metal-support interaction deactivating the Pt. [13]. In contrast, with C_3H_8, changing the support to SiO_2 results in little [12] or no [14] DeNO_x activity being observed. This supports the idea that in the C_3H_8–NO–O_2 reaction NO_x reduction involves reaction on the Al_2O_3. The C_3H_8 light-off occurs at a lower temperature over Pt/SiO_2 compared with a Pt/Al_2O_3 sample of comparable metal dispersion in the same way as observed with C_3H_6, suggesting that the hydrocarbon oxidation, by reaction with O_2 (as opposed to NO_x) occurs exclusively on the metal with both C_3H_6 and C_3H_8. Note that with both C_3H_8 and C_3H_6 the vast majority of the hydrocarbon is oxidised by O_2 and not NO_x.

The effect of catalyst sulphation on the C_3H_6–NO–O_2 and C_3H_8–NO–O_2 reactions over Pt/Al_2O_3 (Figs. 1 and 2, open points) can be understood in terms of the proposed reaction mechanisms. The Pt/Al_2O_3 was sulphated under oxidising conditions, which is expected to result in the formation of sulphate species on the Al_2O_3 support, but not result in any sulphur species being deposited on the metal [15,16]. The C_3H_6–NO–O_2 reaction is unaffected by sulphation, which is then consistent with the reaction occurring only on the Pt surface. In contrast, sulphation results in

the maximum NO_x conversion of the C_3H_8–NO–O_2 reaction falling from 33% to 10%. This is attributed to the blocking by sulphate species of (non-Pt) sites at which NO_x reduction occurs. Note that the fall in NO_x reduction is not due to a lower availability of C_3H_8 as a result of the shift in C_3H_8 light-off since NO_x reduction is observed to be zero order in C_3H_8 for both unsulphated and sulphated Pt/Al_2O_3 [6,17].

The adsorption of NO_x on Al_2O_3 is likely to be important for catalyst/reductant systems in which NO_x reduction occurs on the Al_2O_3. For this reason, TPD of NO_x from Al_2O_3 was studied. The amount of NO_x adsorbed in the absence of O_2 is very much less than that adsorbed in the presence of O_2, suggesting that oxidation of NO, either in the gas phase (i.e. oxidation of NO to NO_2) or after weak adsorption of NO on Al_2O_3 has occurred, is an important step in the adsorption of NO_x. After adsorption of NO+O_2, two NO_x desorption peaks are seen in the TPD. The higher temperature peak coincides with an O_2 desorption suggesting that this peak corresponds to the decomposition of a nitrate species. The lower temperature NO_x desorption peak is not associated with an O_2 desorption and so corresponds to the desorption of some other NO_x species. Literature reports of nitrate species on Al_2O_3 after treatment in NO+O_2 shows the presence of nitrosyl, nitrite and nitrate species on the Al_2O_3 surface [19,20].

Sulphation of the Al_2O_3 to increasing degrees results in a decrease in the high temperature NO_x desorption peak, suggesting that surface sulphate species are able to block the sites at which the proposed nitrate species form on the Al_2O_3. These species, being the conjugate bases of strong acids, would be expected to favour similar sites on the surface, and from our results it is seen that the sulphate species is more strongly bound than the nitrate. For comparison, the decomposition temperatures for bulk aluminium sulphate and aluminium nitrate are 770°C and 150°C [18], respectively, indicating that sulphate species are much more stable that nitrates.

The interaction of C_3H_8 with Al_2O_3 was investigated by temperature programmed (TP) reaction. In the absence of an NO+O_2 pretreatment, C_3H_8 does not adsorb on Al_2O_3, i.e. no uptake of C_3H_8 occurs nor was any carbon found to be deposited on the Al_2O_3 after the experiment. However, if the Al_2O_3 is predosed with NO+O_2, uptake of C_3H_8 is observed at temperatures above 300°C, indicating that C_3H_8 reacts with the adsorbed NO_x. In addition, carbon was found to be deposited on the Al_2O_3 after the experiment (Table 2). The C_3H_8 is oxidised by an adsorbed nitrate species, or more likely several adjacent nitrate species, resulting in the formation of CO and CO_2. This simultaneously reduces the adsorbed nitrate species to a form (e.g. NO or NO_2) which is unstable on the Al_2O_3 surface at these temperatures and which desorbs or is further reduced to N_2. Note that the lower temperature NO_x desorption species are unaffected by the presence of C_3H_8 and that the C_3H_8 level is unaffected by this desorption, indicating that it is only the nitrate species (i.e. the species associated with higher temperature desorption) that can react with C_3H_8. It is speculated that the first step in the C_3H_8–NO–O_2 DeNO_x reaction is the abstraction of a H atom from the C_3H_8 by the basic nitrate group. This mechanism, i.e. the adsorption of NO+O_2 to form a nitrate species, with which C_3H_8 can react is summarised in Fig. 15.

The greater activity in the C_3H_8–NO_2–O_2 reaction (Fig. 4) compared to the C_3H_8–NO–O_2 reaction (Fig. 3) over Al_2O_3 can be understood in terms of this mechanism. The nitrate species on the Al_2O_3, required for activation of the C_3H_8, is expected to be formed more rapidly from NO_2, than from NO+O_2, since NO oxidation, which is likely to be slow over Al_2O_3, is not then required.

The decrease in DeNO_x activity observed in the C_3H_8–NO–O_2 reaction over Al_2O_3 and Pt/Al_2O_3 after sulphation of the catalyst can also be considered in terms of this mechanism. As discussed above, with these reactions NO_x reduction appears to occur via reaction of NO_2 with C_3H_8 on the support and/or at the metal-support interface. Sulphation of the Al_2O_3 results in a decrease in the number of sites available for the nitrate species to be adsorbed (see above) and

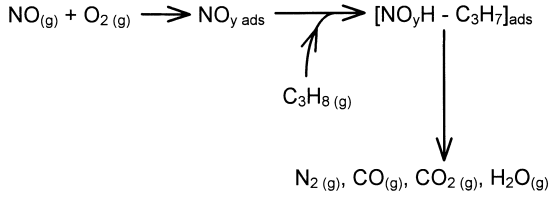

Fig. 15. Proposed mechanism for the C_3H_8–NO–O_2 reaction over Al_2O_3.

hence in the number of adsorbed nitrate species with which C_3H_8 can react, i.e. sulphation blocks the sites at which NO_x reduction occurs. This is illustrated by Fig. 12, which shows that the amount of species with m/e=44 (i.e. CO_2 and N_2O) evolved in a C_3H_8 TP reaction experiment with Al_2O_3 decreases as the degree of sulphation increases. With the reaction over Pt/Al_2O_3 sulphation also increases the activity for C_3H_8 oxidation and hence reduces the availability of reductant for NO_x reduction. However, since NO_x reduction is zero order in C_3H_8 [6,17] the lower availability of reductant is not an important factor. With the reaction over Al_2O_3, sulphation results in depression of C_3H_8 oxidation, presumably because sites for the C_3H_8–O_2 reaction are also blocked by sulphate species.

As discussed above, NO_x reduction in the C_3H_8–NO–O_2 reaction over Pt/Al_2O_3 is believed to occur via migration of NO_2, produced by oxidation of NO to NO_2 on the Pt, onto the metal-support interface where it reacts with C_3H_8, in the same way as in the C_3H_8–NO_2–O_2 reaction over Al_2O_3. However, comparison of these reactions (Figs. 2 and 4) reveals a subtly in the mechanism. With the reaction over Pt/Al_2O_3, NO_x reduction has begun at 250°C, while the C_3H_8–NO_2–O_2 reaction does not start until 375°C. In addition, reaction over Pt/Al_2O_3 produces N_2 and N_2O [6], while reaction over Al_2O_3 produces N_2 but no N_2O. Inaba et al. [14] have also made similar observations on these two reactions.

A possible explanation for this is that with Pt/Al_2O_3 the $DeNO_x$ reaction occurs at the metal-support interface between NO_2 adsorbed either on the Pt at the interface and/or adsorbed at the interface between the Pt and Al_2O_3, and C_3H_8-derived species adsorbed on the Al_2O_3. It may be that the lower temperature required for NO_x reduction is simply the result of a high concentration of NO_2 on the Al_2O_3 at the metal-support interface resulting from the fact that the NO_2 is produced on the Pt surface, this NO_2 coverage being much greater than that obtained on Al_2O_3 alone by adsorption of NO_2 from the gas phase. Alternatively, it may that the interfacial sites are different in nature to those on the rest of the Al_2O_3. The absence of N_2O production with Al_2O_3 (in contrast to Pt/Al_2O_3) may be due to the higher temperature at which NO_x reduction occurs, or it may be that N_2O is only formed at the interfacial sites of Pt/Al_2O_3.

5. Conclusions

Results have been presented for a number of $DeNO_x$ systems with different catalysts and reductants and similarities between these reactions highlighted. In particular, the reasons for differing resistance to sulphur poisoning have been discussed. Knowledge of the reaction mechanism is important when considering how better $DeNO_x$ catalysts might be designed. The mechanisms of the reactions discussed here can be divided into two classes:

1. *Reactions in which* NO_x *reduction occurs exclusively on the* Pt *surface*. The C_3H_6–NO–O_2 reactions over Pt/Al_2O_3 and Pt/SiO_2 are examples of this. This mechanism requires a sufficiently good reductant to keep the metal in a reduced state, i.e. with a negligible oxygen coverage. This type of reaction gives activity at the lowest temperature and is resistant to poisoning by sulphur. Higher activity (lower temperature reaction and higher maximum NO_x conversion) is obtained with non-interacting supports, such as SiO_2. NO_x is reduced to N_2O as well as N_2.
2. $DeNO_x$ *reactions on* Al_2O_3 *with weakly adsorbed reductant*. The C_3H_8–NO–O_2 reaction over Pt/Al_2O_3 and Al_2O_3 and the C_3H_8–NO_2–O_2 reactions over Al_2O_3 are examples of this. These reactions are strongly poisoned by sulphur and appear to occur via the formation of a surface nitrate species on the Al_2O_3 which activates the reductant. This class can be further subdivided into catalysts with and without Pt, the former being active at lower temperature, but producing N_2O as well as N_2.

Acknowledgements

We are grateful to the EPSRC for financial support for this work through grants GR/K01452 and GR/K70403.

References

[1] R. Burch (Ed.), Catal. Today 26 (1995).
[2] M. Iwamoto (Ed.), Catal. Today 22 (1994).
[3] R. Burch, T.C. Watling, Catal. Lett. 37 (1996) 51.
[4] Eight Peak Index of Mass Spectra, 3rd ed., Unwin, Surrey, 1983.

[5] H.C. Yao, H.K. Stepien, H.S. Gandhi, J. Catal. 67 (1981) 231.
[6] R. Burch, T.C. Watling, J. Catal. 196 (1997) 45.
[7] H. Hamada, Catal. Today 22 (1994) 21.
[8] H. Hamada, Y. Kintaichi, M. Tabata, M. Sasaki, T. Ito, Chem. Lett. (1991) 2179.
[9] M. Shimokabe, K. Itoh, N. Takezawa, Catal. Today 36 (1997) 65.
[10] R. Burch, T.C. Watling, in: The Proceedings of the Fourth International Congress on Catalysis and Automotive Pollution Control, CAPoC 4, Brussels, to be published.
[11] R. Burch, P.J. Millington, A.P. Walker, Appl. Catal. B 4 (1994) 65.
[12] R. Burch, T.C. Watling, Catal. Lett. 43 (1997) 19.
[13] C.P. Hubbard, K. Otto, H.S. Gandhi, K.Y.S. Ng, J. Catal. 144 (1993) 484.
[14] M. Inaba, Y. Kintaichi, H. Hamada, Catal. Lett. 36 (1996) 223.
[15] D.D. Beck, M.H. Krueger, D.R. Monroe, SAE Tech. Paper, 910844, 1991.
[16] C. R Apesteguia, T.F. Garetto, A. Borgna, J. Catal. 106 (1987) 73.
[17] R. Burch, T.C. Watling, unpublished results.
[18] Handbook of Chemistry and Physics, 52nd ed., CRC Press, Cleveland, OH, 1971.
[19] V.A. Sadykov, S.L. Baron, V.A. Matyshak, G.M. Alikina, R.V. Bunina, A.Ya. Rozovskii, E.V. Lunin, A.N. Kharlanov, A.S. Ivanova, S.A. Veniaminov, Catal. Lett. 37 (1996) 157.
[20] R. Hierl, H.-P. Urbach, H. Knozinger, J. Chem. Soc. Faraday Trans. 88 (1992) 355.